Journal of Computational Acoustics
© IMACS

ERROR BOUNDS IN MATCHED FIELD INVERSION FOR GEOACOUSTIC PROPERTIES

N.R. CHAPMAN
School of Earth and Ocean Sciences
University of Victoria
Victoria, B.C. V8W 3P6

K.S. OZARD AND M.L. YEREMY
Esquimalt Defence Research Detachment
Defence Research Establishment Atlantic
PO Box 17000 STN FORCES V9A 7N2

Received
Revised

The effect of uncertainty in the parameters that define the experimental geometry is investigated to determine the performance of matched field inversion for geoacoustic properties. The investigation is carried out using simulated data for a vertical line array in a North Pacific environment. The results indicate that there can be significant degradation of inversion performance for small errors (~1/3 wavelength) in source depth, depth and tilt of the array, ocean depth and source/array range. The relatively high sensitivity to mismatch in experimental geometry suggests that uncertainties of this type can be tolerated in the inversion by including the geometrical parameters in the global search algorithm. The simulations show that performance is improved by inverting for both the ocean bottom properties and the geometrical parameters simultaneously.

1. Introduction

Matched Field (MF) inversion is a model-based signal processing technique that has been applied to the estimation of geoacoustic properties, and various investigations, both experimental and theoretical, have recently been reported by several research groups[1-8]. MF inversion is formulated as an optimization problem, and the inversion method is very straightforward. For a known experimental geometry, MF processing is used to invert the acoustic field data in order to determine the properties of the ocean waveguide. The inversion proceeds by specifying a set of geoacoustic models as a basis for calculating replica fields, and then searching the model parameter space to obtain the best correlation between the measured and modeled acoustic fields. The set of geoacoustic model parameter values for which this condition is obtained is defined as the optimum model. The practical application is dependent upon an efficient global search method to search the multidimensional geoacoustic model parameter space for the optimum model. Two methods have generally been employed in ocean acoustics: simulated annealing[1-5] and genetic algorithms[5-7], and a combination of genetic algorithms with a gradient descent process has also been proposed[8].

The performance of MF inversion for estimation of geoacoustic properties is affected by many factors that can generally be grouped into two basic types. The first type includes the components of the numerical algorithm such as the type of MF processor, the acoustic propagation model, and the form of the geoacoustic model, and the second type includes experimental factors such as the data quality and uncertainty in the experimental geometry. Although the geometry in a MF inversion experiment is assumed to be known, some degree of error exists in the measurements made to define the source and receiver locations. In

this paper we investigate the effect of uncertainties in the experimental geometry on the performance of a MF inversion algorithm based on a Bartlett MF processor and a vertical line array (VLA). Errors in the parameters that define the experimental configuration are manifested in the inversion as mismatch. In general, the inversion performance is sensitive to mismatch in quantities such as range, ocean depth, source depth, and array depth and tilt. These are quantities that are measured independently in MF inversion experiments in order to establish the experimental geometry, and they constitute the set of parameters investigated in this paper. The sound speed profile in the water is assumed to be known; this quantity is usually measured with high precision in experiments to define the environment at the site.

The effect of geometrical mismatch was investigated by means of a simulation study for a VLA in a range-independent ocean waveguide in which the bottom was modelled as a fluid sediment layer over an elastic basement. Studies have also been carried out analytically to determine the effect of parameters such as range and ocean depth[9], but the use of simulated data determines specific information for an experimental environment, and also provides indications for more general behaviour. The environment and experimental geometry were chosen to simulate the conditions at the site of one of the PACIFIC ECHO experiments in the Northeast Pacific[10]. Inversions were carried out using replica fields that were calculated for known amounts of error in the geometrical parameters. Both the MF correlation (i.e., the output of the Bartlett processor) and the deviation from the true model parameter values were used as measures of the inversion performance. The relatively high sensitivity to mismatch due to uncertainties in the experimental geometry suggests that the errors can be tolerated in the inversion by including geometrical parameters in the global search process. This simple application of the concept of focalization[11] was investigated in the study. However, since the geometrical parameters are often strongly correlated, we have considered the effect of each parameter on an individual basis.

In the remainder of this paper, the matched field inversion method is outlined and the environment for the simulation study is described. Following this, the results obtained for the effect of geometrical errors on inversion performance are presented, and the use of focalization as a means for tolerating and exploiting the errors is discussed.

2. Matched Field Inversion Method

The basic components of a matched field inversion algorithm have been described previously[1,2]. The components of the method employed in this work are discussed in this section.

The cost function, $B(m)$, for the MF inversion algorithm is based on the Bartlett MF processor, which describes the correlation between measured and modelled acoustic fields. This function is defined as

$$B(m) = p^*(m)Rp(m) \tag{1.1}$$

where $p(m)$ is the field calculated for a specific environmental model m, and R is the cross spectral matrix of the measured field, X. Although the Bartlett processor has low resolution and high sidelobes, it is robust to conditions of mismatch and noise, and is thus appropriate for searching the model parameter space. The modelled fields were calculated using the normal mode method KRAKENC[12]. This model calculates the discrete complex wavenumbers corresponding to the propagating modes in an elastic waveguide, and is suitable for the geoacoustic model used in this study.

The geoacoustic model consists of three layers: a water layer, a relatively thin fluid homogeneous sediment layer of thickness h, and an elastic basement half-space. The sediment is described by its sound speed, density and attenuation; the basement is described by the compressional (p) and shear (s) speeds and

attenuations, and the density. The model is typical of thin-sediment, very young oceanic crust environments in the Pacific.

A simulated annealing algorithm[13] was used to search the model parameter space in order to estimate the geoacoustic parameters. Since the inversion is sensitive to the similarity between the measured and modelled acoustic fields at the array, it is possible that a high MF correlation could be obtained for an entirely unrealistic set of geoacoustic model parameters. In order to minimize the likelihood of this outcome, reasonable bounds for the model parameter values were selected based on *a priori* knowledge of the geoacoustic environment. The search was initiated with random values chosen within the imposed bounds; the inversion then proceeded through a series of iterations involving random perturbations of the model parameters while a control parameter, analogous to the temperature, was reduced. Perturbations that increased the cost function were accepted unconditionally, whereas those that decreased the cost function were accepted according to an acceptance probability given by the Boltzmann distribution,

$$P(\Delta B_i) = \exp(\frac{\Delta B_i}{s_i T}) \tag{1.2}$$

Here, s_i is a scale factor for the ith model parameter and T is the control parameter. The scale factor accounts for the different sensitivities of the model parameters, so that all parameters converge at about the same rate, analgous to the cooling of a mixture[1].

The selection of the cooling schedule to obtain convergence of the annealing process is, in general, a trial and error exercise that requires experience to judge how many iterations are necessary to provide adequate sampling of the parameter values[14]. Thus, the cooling schedule is specific to the dimensionality and landscape of each particular model parameter space. In this work, the temperature was reduced according to the exponential cooling schedule given by

$$T_{j+1} = \gamma^{j+1} T_0, \text{ with } \gamma \leq 1 \text{ and } j = 0,1... \tag{1.3}$$

The starting temperature, T_0, was determined by observing several short MF runs with different initial temperatures in order to select a value that provided sufficient freedom in the initial stages to investigate all regions of the parameter space, analgous to a melted state. Previous work has indicated that an acceptance of 80-85% of all model perturbations corresponds to a sufficiently melted state. The number of iterations was estimated by calculating the temperature at which the acceptance criterion excluded any changes greater than a preset value of the tolerable error. The model parameter values were perturbed according to the expression

$$m_{i+1} = m_i + \varepsilon^3 \delta_i \tag{1.4}$$

where ε is a random number from a uniform distribution on [-1,1], and δ_i is the maximum perturbation for the ith parameter[1,3]. This distribution approximates a Cauchy distribution, and is considered to be more effective than a Gaussian schedule in searching the parameter space because it provides a greater chance of making large changes in parameter values, while at the same time ensuring that most changes are small.

3. Simulations

3.1. *Environment*

The simulations were carried out for a VLA in the ocean environment shown in Figure 1. The sound speed profile for the water column was a North Pacific profile that was truncated at 1000 m. The profile was limited in depth in order to reduce the number of propagating modes, and consequently minimize the time required for calculating the replica vectors in the global search process. The essential feature of the profile, the sound speed minimum, is preserved, but the resulting environment is somewhat more bottom limited than the actual environment. The ocean bottom consisted of two homogeneous layers: a sediment layer 75 m thick, with density 1.8 g/cm^3, sound speed 1600 m/s and attenuation 0.2 dB/λ, and an elastic basement with density 2.4 g/cm^3, p-wave speed 2700 m/s, s-wave speed 1250 m/s, and both attenuations 0.1 dB/λ.

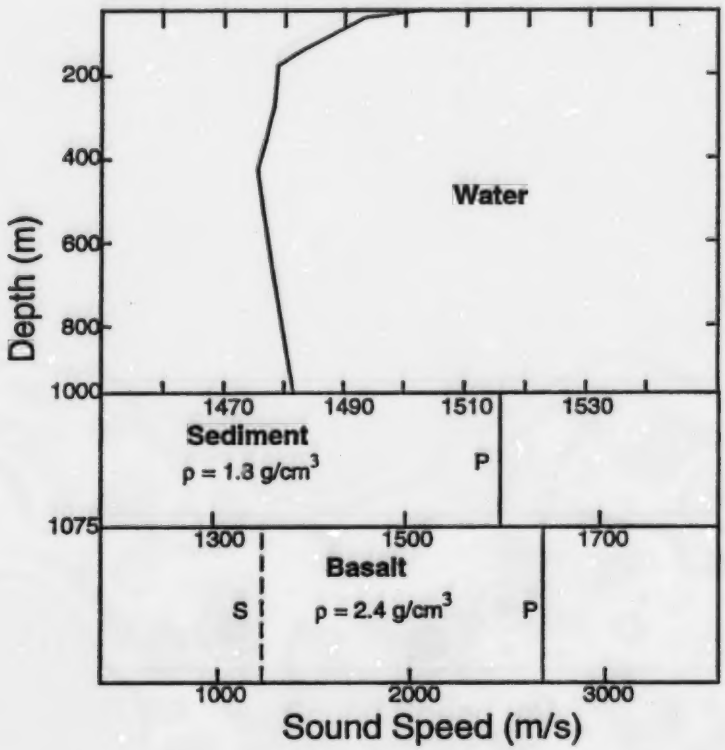

Figure 1. Sound speed profile for the North Pacific simulation environment. The geoacoustic model consists of a relatively thin fluid sediment overlying an elastic basement.

The VLA consisted of 16 hydrophones spaced at 40 m, with the topmost element at a depth of 200 m. The array was located at a range of 2 km from a 10-Hz source at a depth of 46 m. This geometry simulated the experimental arrangement in one of the PACIFIC ECHO sea trials that was carried out near

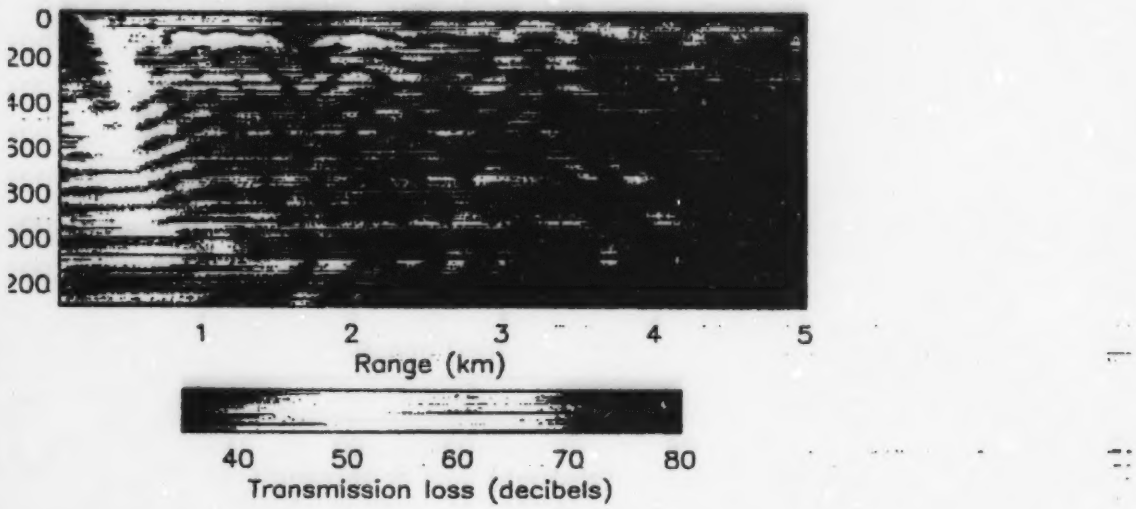
0
200
400
300
300
000
200
1
2
3
4
5
Range (km)
40
50
60
70
80
Transmission loss (decibels)

the Juan de Fuca ridge in the North Pacific[10]. For these conditions, there were 14 modes. The KRAKENC[12] solutions were benchmarked against SAFARI[15] calculations to confirm that the code was indeed satisfactory for this environment. The acoustic field for the 46-m source is shown in Figure 2.

Figure 2. Acoustic field for the 10-Hz CW source operating at a depth of 46 m in the North Pacific environment shown in Figure 1.

3.2. *Parameter sensitivities*

Initially the model parameter sensitivities were investigated in order to determine the temperature scale factors. Each parameter was tested separately by varying its value over the allowed range while all others were fixed at their true values in calculations of the cost function. A hierarchy in sensitivity was observed, with fluid layer depth and basement p-wave speed the most sensitive, and the sediment layer sound speed and basement s-wave speed moderately sensitive. The least sensitive parameters were the densities and the attenuations. Similar tests carried out for the geometrical parameters indicated that the sensitivities for the ocean depth and array depth were equivalent to those for the most sensitive geoacoustic model parameters; the range was somewhat less sensitive.

Examples of the parameter sensitivites are shown in Figure 3 where the cost function is plotted over a mismatch range of $\pm$ 20 % of the true value for four of the model parameters. Each component of the figure represents a one-dimensional slice of the parameter space. The correlations span the full range of values for the basalt p-wave speed and the sediment depth; the basalt s-wave speed is about ten times less

sensitive, and the density is about 100 times less sensitive than the most sensitive parameters. Based on the results of this study, the inversion searched for the values of the six bottom parameters listed in Table 1; the attenuations were held at fixed values.

The model parameters were assigned the scale factors indicated in Table 1. The use of scale factors generally improves the inversion performance; not only are the estimates improved for those parameters that have the least effect on the acoustic field but also the errors for the more sensitive parameters are reduced. For example, the annealing process tends to compensate for an error in density by adjusting the sound speed in order to obtain the correct impedance. The scale factors were held at fixed values throughout the inversion; experience has indicated that although the parameter sensitivities varied significantly from the initial to the final parameter set, the hierarchy of sensitivities was maintained during the annealing process.

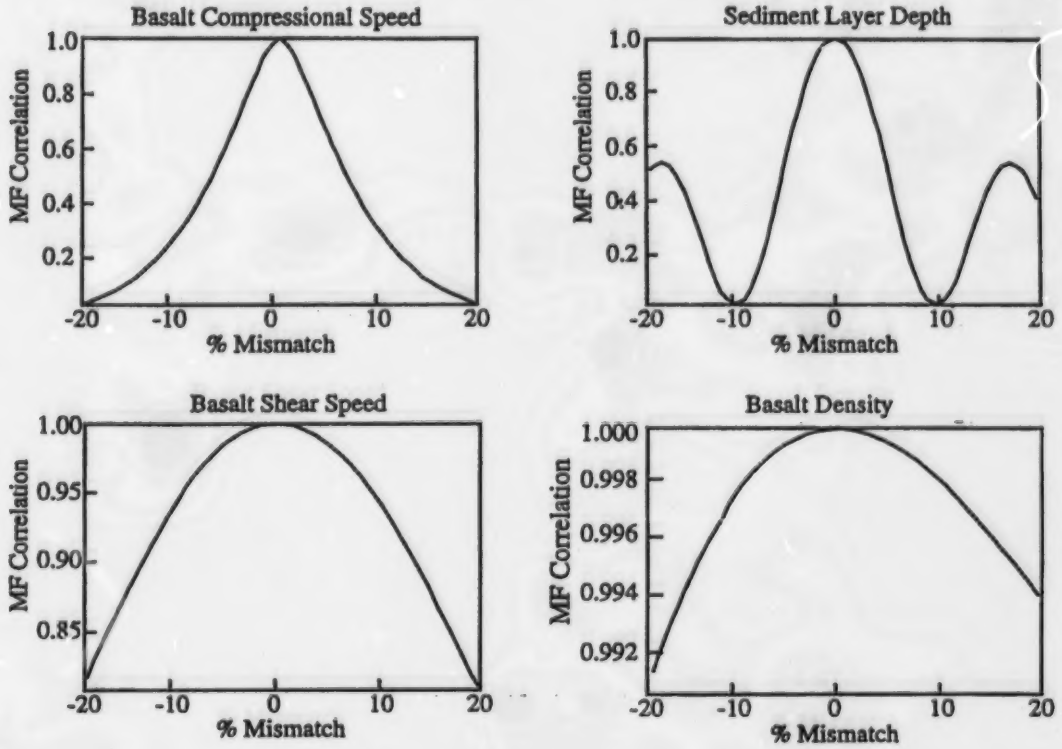

Figure 3. Parameter sensitivities for the basalt p-wave speed, sediment layer depth, basalt s-wave speed and the basalt density. The scale of sensitivity is indicated by the range of MF correlation values over the ± 20 % mismatch variation. The full range is [0,1].

An inversion was carried out for the ideal case of no geometrical mismatch in order to verify the method. The annealing schedule for this inversion and all the other tests consisted of 1000 iterations, initiated with values of $T_0 = 2.0$, and $\gamma = 0.9988$. The final estimates for each parameter are listed in Table 1, along with the true values, the search ranges and the scale factors

The MF correlation (i.e., the output of the Bartlett processor) and the deviation from the true model parameter values were used as measures of the inversion performance. The final value of the Bartlett

MF power was 0.9999, and the estimated values are in very close agreement with the true values; errors for even the less sensitive parameters are less than 2 %. The cooling curve is shown in Figure 4, where the cost function for accepted models is plotted versus iteration number. There is roughly equal acceptance of increasing and decreasing models for about the first 4000 iterations, but subsequently the Bartlett MF power increases to a value close to unity. The annealing curves for selected parameters are shown in Figure 5, where the accepted parameter values are plotted versus iteration number. These curves show that the allowed range of values was adequately searched in the initial stages of the annealing process when the temperature was high.

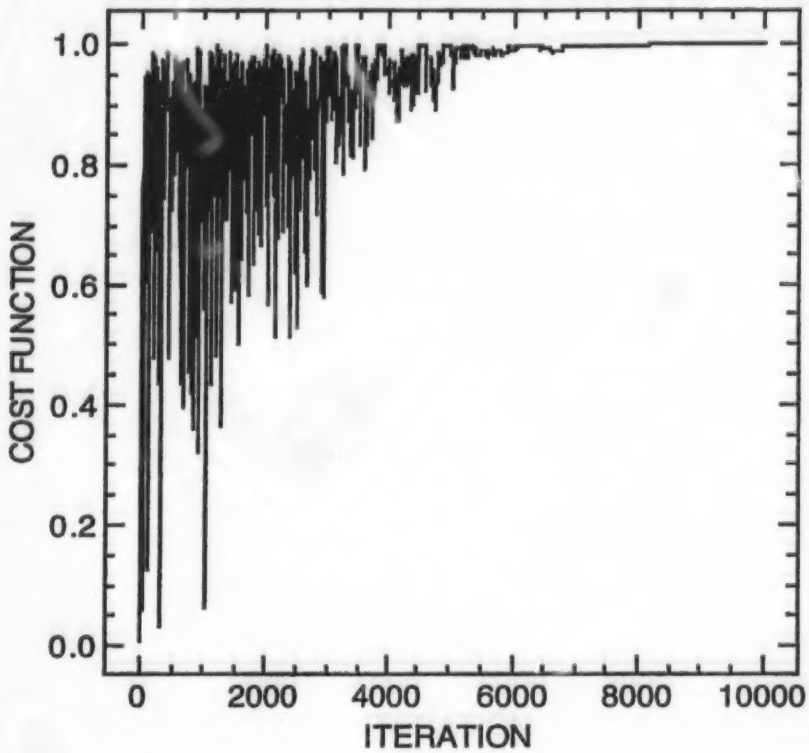

Figure 4. Cost function for the ideal inversion with no geometrical mismatch.

Table 1. Results for ideal case: no geometrical mismatch. The final value for the cost function is 0.9999.

Parameter	True	Limits	s	Estimate
h (m)	75	(50-100)	1.0	77.3
c_1 (km/s)	1.6	(1.4 - 1.7)	10.0	1.61
ρ_1 (g/m^3)	1.55	(1.3 - 2.0)	100.0	1.55
c_{2p} (km/s)	2.7	(2.5 - 2.9)	1.0	2.68
c_{2s} (km/s)	1.25	(1.05 - 1.45)	10.0	1.25
ρ_2 (g/m^3)	2.4	(2.1 - 2.7)	100.0	2.54

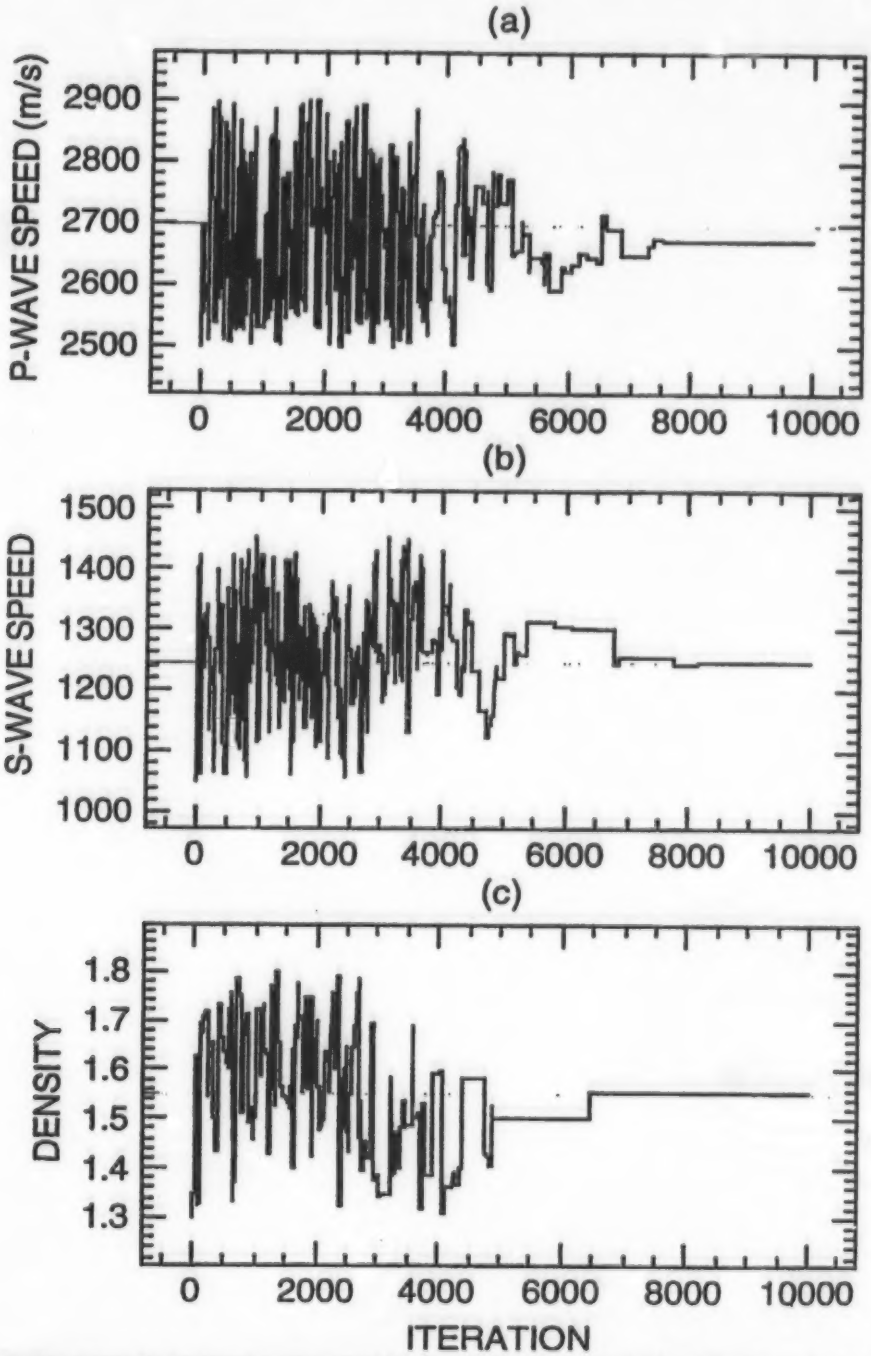

Figure 5. Cooling curves for basement p-wave speed (a), basement s-wave speed (b) and fluid layer density (c). The true values for these parameters are shown by the light horizontal lines.

3.3. *Range error*

The investigation for the effect of mismatch in range was carried out using simulated data for the true range, and then calculating replica fields for ranges that were displaced from the true range by a known fraction of the acoustic wavelength, λ. The parameter search ranges were the same as those listed in Table 1. The results are shown in Table 2 for range errors from -4/3 λ to 4/3 λ in steps of 1/3 λ. The model parameter estimates are good for the relatively small error of 1/3 λ, and the estimates for the other parameters are acceptable. However, for greater errors the cost function decreases significantly and the errors in the most sensitive parameters are large (10 -20 %). For this environment, there is an asymmetry depending on whether the assumed ranges were less than or greater than the true range. This behavior reflects the structure of the acoustic field near the array, and is not likely a general result. The final column in the table shows the results of including range as a search parameter, within the bounds of ± 2/3 λ (± 100 m). The effect is remarkable; the range is recovered to within 1% and all the geoacoustic parameters are estimated accurately, with a final Bartlett power of 0.9984.

Table 2. Effect of error in range on MF Inversion performance.

Parameter	-4/3 λ	-2/3 λ	-1/3 λ	1/3 λ	2/3 λ	4/3 λ	Range Search
h (m)	69.0	70.7	73.7	67.0	59.3	62.6	76.8
c_1 (km/s)	1.42	1.74	1.71	1.61	1.53	1.61	1.57
ρ_1 (g/m^3)	1.32	1.34	1.30	1.62	1.68	1.31	1.64
c_{2p} (km/s)	2.50	2.89	2.73	2.75	2.89	2.89	2.69
c_{2s} (km/s)	1.39	1.33	1.30	1.10	1.26	1.44	1.24
ρ_2 (g/m^3)	2.51	2.54	2.62	2.15	2.44	2.62	2.26
Range							2.016
Cost Function	0.854	0.899	0.985	0.953	0.8475	0.724	0.998

3.4. *Array/source depth error*

The investigations of the effects of mismatch in array and source depths were carried out in a similar fashion, using replica fields with depths that were displaced from the true depths by a known fraction of the wavelength. The results for array depth are presented in Table 3 for depth errors from -1/3 λ to 2/3 λ. The model parameter estimates are acceptable for relatively small errors (<1/3 λ), but for greater errors the performance degrades, as observed for the effect of range. The final column in Table 3 shows the results of including array depth as a search parameter, within the bounds of ± 20 m (~ 1/6 λ) referenced to the top hydrophone at a depth of 200 m. As observed with the range search, the depth is recovered to within 1% and all the geoacoustic parameters are estimated accurately. Similar behaviour is shown in Table 4 for the effect of source depth; negative changes (relative to a wavelength) are not calculated in this case since the source depth is within a wavelength of the surface. Also, since there is a symmetry between the source and array depths, the source depth was not searched. Both the array and source depth errors are more sensitive than range errors, as expected for the VLA geometry.

Table 3. Effect of array depth errors on MF inversion performance

Parameter	-1/3λ	-1/6 λ	1/6 λ	1/3λ	2/3 λ	Depth Search
h (m)	62.8	81.9	66.0	62.9	64.9	75.7
c_1 (km/s)	1.80	1.78	1.46	1.44	1.44	1.62
ρ_1 (g/m^3)	1.30	1.49	1.68	1.38	1.40	1.55
c_{2p} (km/s)	2.85	2.78	2.66	2.64	2.58	2.68
c_{2s} (km/s)	1.21	1.45	1.11	1.08	1.39	1.27
ρ_2 (g/m^3)	2.16	2.24	2.17	2.15	2.63	2.50
Array Depth (m)						198.3
Cost Function	0.659	0.851	0.906	0.765	0.665	0.999

Table 4. Effect of source depth errors on MF inversion performance.

Parameter	1/6 λ	1/3λ	2/3 λ
h (m)	80.7	73.4	64.9
c_1 (km/s)	1.63	1.74	1.42
ρ_1 (g/m^3)	1.69	1.71	1.30
c_{2p} (km/s)	2.82	2.84	2.55
c_{2s} (km/s)	1.17	1.09	1.32
ρ_2 (g/m^3)	2.61	2.42	2.57
Cost Function	0.963	0.725	0.641

3.5. *Array tilt error*

The combined errors in array depth and range are manifested as array tilt. This quantity is usually measured in experiments, and the effect of tilt is particularly important in shallow water where the currents are generally much stronger than in deep water, and can cause significant tilts. The effect of array tilt was investigated here for values of 3° and 14°, and the results are shown in Table 5. For the latter tilt, the error in array range at the bottom of the array was about 170 m, and the degradation in performance is roughly equivalent to that for a range error of about a wavelength and an array depth error of ~ 1/6 λ. Searching over tilt between the limits of 1.5 -4.5 ° for an array tilted at an angle of 3.0° provides a significant improvement, as indicated in the final column of the table, and the tilt angle itself is recovered to within 5%.

Table 5. Effect of errors in array tilt on MF Inversion performance.

Parameter	3°	14°	Tilt Search
h (m)	71.6	90.3	77.2
c_1 (km/s)	1.64	1.70	1.78
ρ_1 (g/m^3)	1.61	1.94	1.55
c_{2p} (km/s)	2.76	2.86	2.81
c_{2s} (km/s)	1.30	1.09	1.13
ρ_2 (g/m^3)	2.42	2.29	2.52
Array Tilt			3.1°
Cost Function	0.924	0.828	0.999

3.6. Ocean depth error

The effect of mismatch in ocean depth was carried out in a similar fashion, and the results are shown in Table 6. Although this quantity is not strictly speaking a geometrical parameter, the ocean depth is generally measured in experiments in an attempt to establish the experimental arrangement. The impact of an error in this parameter is considerably more severe, as observed in the table by the decrease in the cost function to values < 0.4 for depth errors of 2/3 λ. This result is not unexpected since the modal structure is strongly sensitive to the waveguide depth. The cost function decreases significantly for changes as large as 1/3 λ, and the errors in the estimated values of the geoacoustic parameters are generally greater than 20%. However, including the depth as a search parameter in the inversion (using limits within ± 100 m of the true value) provides considerable improvement in the estimates of all parameters.

Table 6. Effect of ocean depth errors on MF inversion performance.

Parameter	-1/3λ	-1/6 λ	1/6 λ	1/3λ	2/3 λ	Depth Search
h (m)	77.9	86.3	64.2	54.4	99.7	75.5
c_1 (km/s)	1.41	1.51	1.72	1.69	1.59	1.59
ρ_1 (g/m^3)	1.34	1.77	1.33	1.76	1.83	1.59
c_{2p} (km/s)	2.87	2.66	2.79	2.76	2.89	2.71
c_{2s} (km/s)	1.07	1.31	1.29	1.06	1.17	1.24
ρ_2 (g/m^3)	2.33	2.19	2.37	2.59	2.59	2.38
Depth (km)						0.999
Cost Function	0.597	0.747	0.703	0.617	0.381	0.999

3.7. *General remarks*

The relative importance of the various types of mismatch can be inferred from Figure 6, where the final cost function values for all the parameters tested are plotted versus relative error. For this environment, the inversion is least sensitive to range mismatch and significantly more sensitive to mismatch in ocean depth; sensitivity to array/source depth mismatch is intermediate. These results are consistent with the behavior expected for a VLA. However, the effect on estimates of the individual geoacoustic parameters is not immediately apparent from an analysis of the cost function alone. From the information in Tables 2-6, the estimates for the most sensitive geoacoustic parameters are not strongly affected by small errors in experimental geometry. Also, there appears to be no bias in the estimates depending on the sign of the error in the geometrical parameter. In contrast, generally strong correlation has been observed in other studies between estimates of geometrical parameters such as range and ocean depth.

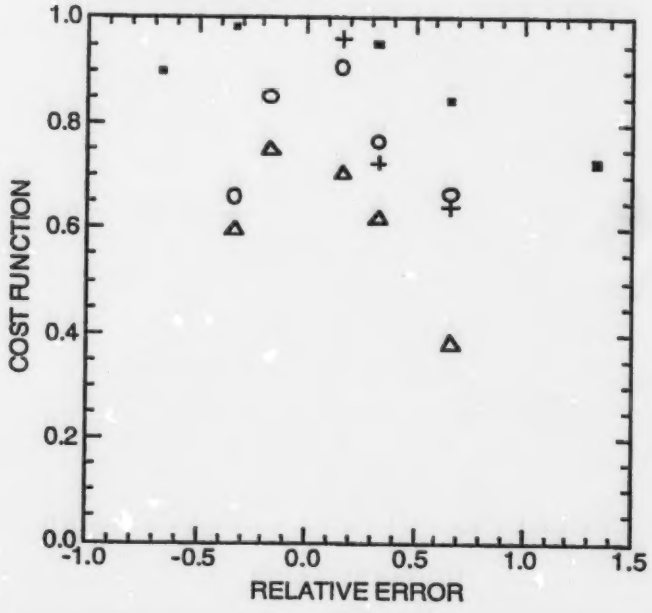

Figure 6. Final values of cost function versus relative mismatch in range (squares), array depth (circles), source depth (crosses) and ocean depth (triangles).

4. Summary

A simulation study was carried out to investigate the effect of geometrical mismatch on geoacoustic inversion performance. The experimental geometry for the simulation was a VLA operating in a North Pacific environment, and a 10-Hz CW sound source. MF inversion based on a simulated annealing search process were performed using replica fields that were mismatched by a known error in one specific geometrical parameter. the general observations on inversion performance were:

- the cost function decreases for increasing geometrical error. Depending upon the specific parameter, there was significant decorrelation for an error of 2/3 λ.

- the most sensitive geoacoustic parameters are robust to small geometrical mismatch (errors < 1/3 λ). However, estimation performance degrades for less sensitive parameters, and the estimates of these parameters are not accurate.

- for large geometrical errors (> 1/3 λ) inversion performance degrades for all parameters.

- including geometrical parameters in the global search process greatly reduces the effect of mismatch in the specific parameter. This application of focalization improved the inversion performance, and provided a method for tolerating geometrical errors in teh inversion. However, since the geometrical parameters can be strongly correlated, expanding the search to include several parameters may not be productive.

Acknowledgements

Work supported by a research partnership program between the Department of National Defence and the Natural Sciences and Engineering Research Council of Canada.

References

1. M.D. Collins, W.A. Kuperman and H. Schmidt, 'Nonlinear inversion for ocean bottom properties', J. Acoust. Soc. Amer., 92, 2770-2783, 1992.
2. C.E. Lindsay and N.R. Chapman, 'Matched field inversion for geoacoustic model parameters using adaptive simulated annealing', IEEE J. Oceanic Eng. 18, 224-231, 1993.
3. N.R. Chapman, and K.S. Ozard, Matched field inversion for geoacoustic properties of young ocean crust, in *Full Field Inversion Methods in Ocean and Seismo-Acoustics*, O. Diachok et al, editors, Kluwer Academic Publishers, Dordrecht, pp 165-170 (1995).
4. N.R. Chapman and C.E. Lindsay, 'Matched-field inversion for geoacoustic model parameters in shallow water', IEEE J. Oceanic Eng. 21, 347-355, 1996.
5. Z-H Michalopoulou, H. Martynov, and M.B. Porter, 'Simulated annealing and genetic algorithms for broadband source focalization', in *Proceedings of the 3rd European conference on Underwater Acoustics*, J. Papadakis, editor, Crete University Press, Heraklion, pp409-414, 1996.
6. P. Gerstoft, 'Global inversion by genetic algorithms for both source position and environmental parameters', J. Comput. Acoust. 2, 251-266, 1994.
7. D.F. Gingras and P. Gerstoft, 'Inversion for geometric and geoacoustic parameters in shallow water: experimental results', J. Acoust. Soc. Am., 97, 3589-3598, 1995.
8. P. Gerstoft, 'Inversion of seismo-acoustic data using genetic algorithms and a posteriori probability distributions', J. Acoust. Soc. Am., 95, 770-782, 1994.
9. E.C. Shang and Y.Y Wang, 'Environmental mismatching effects on source localization processing in mode space', J. Acoust. Soc. Am., 89, 2285-2290, 1991.
10. J.A. Fawcett, M.L. Yeremy and N.R. Chapman, 'Matched field source localization in a range dependent environment', J. Acoust. Soc. Am., 99, 272-282, 1996.
11. M.D. Collins and W.A. Kuperman, 'Focalization: Environmental focussing and source localization', J. Acoust. Soc. Amer., 90, 1410-1422, 1990.
12. M.B. Porter, 'The KRAKEN normal mode program', SACLANT Undersea Research Centre Memorandum. (SM-245), 1991.
13. S. Kirkpatrick, C.D. Gelatt, Jr., and M.P. Vecchi, 'Optimization by simulated annealing', Science, 220, 671-680, 1983.
14. A. Basu and L.N. Fraser, 'Rapid determination of the critical temperature in simulated annealing', Science, 249, 1409-1412, 1990.
15. H. Schmidt, 'SAFARI: Seismo-acoustic fast field algorithm for range-independent environments' SACLANT Undersea Research Centre Report SR-113, 1988.